

to-volume ratios, afford further routes for the design of responsive materials. Functionalized ligands can be placed on the surface of gold or cadmium selenide nanoparticles. Such functional particles can be tethered to the base of the nanopores in thin-film arrays made from diblock copolymer templates. The conformation of the tethering chains will depend on the local solvent environment. Changing the pH, temperature, or solvent quality within the pores causes the chain to stretch or compress, allowing the nanoparticles to move up and down in the pores, exposing or hiding the interacting sites on the nanoparticles and trapping or repelling foreign materials approaching the surface.

A wide range of external stimuli can be used to invoke a specific response from polymeric materials. This has given and will give rise to a broad spectrum of applications, ranging from melt-processing aids to biocompatible materials to chemical sensors. The

unique characteristics of long-chain molecules offer a myriad of possibilities for playing with the chemistry, conformation, and dynamics of the chains to build in specific responses with well-defined response times and triggers, which are key elements in the fabrication of responsive materials.

References and Notes

1. J. Genzer, K. Efimenko, *Science* **290**, 2130 (2000).
2. S. Kongtong, G. S. Ferguson, *J. Am. Chem. Soc.* **124**, 7254 (2002).
3. A. Falsafi, M. Tirrell, A. V. Pocius, *Langmuir* **16**, 1816 (2000).
4. S. K. Thanawala, M. K. Chaudhury, *Langmuir* **16**, 1256 (2000).
5. A. Vaidya, M. K. Chaudhury, *J. Coll. Interface Sci.* **249**, 235 (2002).
6. M. K. Chaudhury, G. M. Whitesides, *Science* **256**, 1539 (1992).
7. C. S. Henkee, E. L. Thomas, L. J. Feter, *J. Mat. Sci.* **23**, 1685 (1988).
8. G. Coulon, V. Deline, P. F. Green, T. P. Russell, *Macromolecules* **22**, 2581 (1989).
9. S. H. Anastasiadis, S. K. Satija, C. F. Majkrzak, T. P. Russell, *J. Chem. Phys.* **92**, 5677 (1990).

10. H. Mori, A. Hirao, S. Nakahama, K. Senshu, *Macromolecules* **27**, 4093 (1994).
11. K. Senshu *et al.*, *Langmuir* **15**, 1754 (1999).
12. G. de Crevoisier, P. Fabre, J.-M. Corpart, L. Leibler, *Science* **285**, 1246 (1999).
13. D. N. Theodorou, *Macromolecules* **21**, 1422 (1988).
14. Y. Hong *et al.*, *Polymer* **41**, 7705 (2000).
15. Y. Hong *et al.*, *J. Rheol.* **43**, 781 (1999).
16. J. F. Hester, P. Banerjee, A. M. Mayes, *Macromolecules* **32**, 1643 (1999).
17. P. Banerjee, D. J. Irvine, A. M. Mayes, L. G. Griffith, *J. Biomed. Mat. Res.* **50**, 331 (2000).
18. D. J. Irvine, A.-V. G. Ruzette, A. M. Mayes, L. G. Griffith, *Biomacromolecules* **2**, 545 (2001).
19. D. G. Walton *et al.*, *Macromolecules* **30**, 6947 (1997).
20. K. Ichimura, S.-K. Oh, M. Nakagawa, *Science* **288**, 1624 (2000).
21. J. P. Penelle, J. Goldbach, T. P. Russell, *Macromolecules* **35**, 329 (2002).
22. T. E. Karis, Y. Gallot, A. M. Mayes, *Nature* **368**, 329 (1994).
23. A.-V. Ruzette *et al.*, *Macromolecules* **31**, 8509 (1998).
24. M. Pollard *et al.*, *Macromolecules* **31**, 493 (1998).
25. A.-V. Ruzette, P. Banerjee, A. M. Mayes, T. P. Russell, *J. Chem. Phys.* **41**, 525 (1990).
26. I would like to acknowledge enjoyable discussions with R. J. Farris at the University of Massachusetts, who knows an awful lot about rubber.

REVIEW

Polymer Vesicles

Dennis E. Discher^{1*} and Adi Eisenberg²

Vesicles are microscopic sacs that enclose a volume with a molecularly thin membrane. The membranes are generally self-directed assemblies of amphiphilic molecules with a dual hydrophilic-hydrophobic character. Biological amphiphiles form vesicles central to cell function and are principally lipids of molecular weight less than 1 kilodalton. Block copolymers that mimic lipid amphiphilicity can also self-assemble into vesicles in dilute solution, but polymer molecular weights can be orders of magnitude greater than those of lipids. Structural features of vesicles, as well as properties including stability, fluidity, and intermembrane dynamics, are greatly influenced by characteristics of the polymers. Future applications of polymer vesicles will rely on exploiting unique property-performance relations, but results to date already underscore the fact that biologically derived vesicles are but a small subset of what is physically and chemically possible.

Vesicles and biomembranes have existed since the first cells and play critical roles in compartmentalization functions as varied as nutrient transport and DNA protection (1). Whereas phospholipids are the natural amphiphiles of cell membranes, vesicle-forming materials used in products ranging from cosmetics to anticancer agents can be synthetic as well as biological [e.g., (2)]. When suitably mixed in water or similar solvents, the oily parts of the amphiphiles tend to associate while the more hydrophilic parts face inner and outer solutions, helping to delimit the

two interfaces of the membrane (Fig. 1A).

Despite the molecularly thin nature of these membranes, the vesicles that form by the relatively weak solvent-associated forces can effectively entrap dissolved compounds and can also accumulate, within the membrane cores, hydrophobic or fatty substances. Several skin-rejuvenating products, for example, not only encapsulate the water-soluble antioxidant vitamin C within lipid vesicles but also dissolve skin-healing vitamin E within the cores. Aggregation of more than 100,000 small amphiphiles such as lipids (with molecular weight $MW < 1$ kD) into the molecularly thin membranes also manifests itself in a dynamic, physical softness (1). As a consequence, many lipid vesicle properties such as encapsulant retention, membrane stability, and degradation are not particularly well controlled.

A polymer approach to vesicle formation—as summarized in this review—broadens the range of properties achievable through a widened choice of amphiphile MW and chemistry. To be clear, the systems reviewed are not polymerized vesicles in which amphiphiles are polymerized or cross-linked after vesicle formation; such an approach has generally started with lipid-size, reactive amphiphiles, and (if successful) generates membranes of the same basic architecture as lipid bilayers (3, 4). Instead, the focus here is on linear polymers with the intrinsic ability to self-direct their own assembly into membranes. Being lipid-like only in the latter sense, vesicle-forming polymers offer fundamental insight into natural design principles for biomembranes.

From archaeobacteria to humans, cell membranes are self-assemblies of lipids (Fig. 1A, a) as well as integrated and peripheral membrane proteins (i.e., large and structured biopolymers). Since Bangham's 1960s description of lipid vesicles or "liposomes" (5), extraction and reconstitution of many such biomembrane systems has led to fundamental as well as technological advances. One example of note is the formation of HIV-like "viroosomes" that have been made by integrating the cell-binding HIV protein gp160 into liposomes (6). A number of highly diverse synthetic systems have also been inspired, starting with 1970s "niosomes" (7) made from nonionic amphiphiles similar in size to lipids. From polyethylene glycol (PEG)–

¹School of Engineering and Applied Science, University of Pennsylvania, Philadelphia, PA 19104–6393, USA. ²Department of Chemistry, McGill University, Montreal, Quebec H3A 2K6, Canada.

*To whom correspondence should be addressed. E-mail: discher@seas.upenn.edu

modified lipids in the 1980s (2) to more recent vesicle-forming species, the solution-dependent surfactant or amphiphilic character of the molecules stands out as having a dominant role in vesicle formation. Examples include a fullerene-based surfactant (8), amphiphilic dendrimers (9), charge-balancing mixtures of cationic and anionic surfactants [e.g., (10)], and various amphiphilic block copolymers (e.g., Fig. 1A, b to d).

Block copolymers have the same basic architecture as lipids but consist of distinct polymer chains covalently linked in a series of two or more segments (11–13). In the absence of any solvent, block copolymers are known to display a wide range of ordered morphologies, including lamellar phases with the same symmetry as a stack of paper. The transition to phases such as the lamellar phase from an isotropically disordered state depends on at least three key parameters of the block copolymers: the overall average MW of the polymer, the mass or volume fraction f of each block, and the effective interaction energy ϵ between monomers in the blocks. These parameters remain key as solvent is added and block copolymer nanostructures swell, rearrange, and transform as lyotropic phases (14, 15). A principal goal of this review is to illustrate how the same molecular properties enter into the formation and emergent properties of block copolymer vesicles in the highly dilute limit.

Vesicles and Micelles As Self-Directed Assemblies

Although swollen lamellar phases can be considered antecedent to diluted vesicles (with a portion of each lamellar sheet becoming a closed encapsulating membrane, as illustrated below), vesicles are also closely related to rod-like and spherical micelle morphologies in that all are solvent-dependent, self-directed assemblies (Fig. 1, B and C). Micelles have been widely reported for many lipid-size surfactants (16) as well as much

larger polymeric superamphiphiles (14, 15, 17). However, micelles strictly lack the shell-like character and encapsulated bulk solution phase of a vesicle.

For a simple amphiphile like a lipid or a diblock copolymer in an aqueous solution, a

time-average molecular shape in the form of a cylinder, wedge, or cone dictates whether membrane, rod-like, or spherical morphologies will respectively form (16). This average molecular shape is most simply a reflection of the hydrophilic-to-hydrophobic ratio f . Il-

lustrative of such geometric forces at work is the behavior of lipids when conjugated at the hydrophilic “head” group with PEG chains (equivalent to polyethylene oxide, PEO). As a fluctuating and hydrated polymer, the typical PEG used [$MW \sim 2$ to 5 kD (2)] leads to a conically shaped amphiphile distinct in form from cylindrically shaped phospholipids. Consequently, phospholipid membranes mixed with sufficient concentrations of PEG-lipid tend to generate the highly curved micelles of Fig. 1, B and C (18).

Despite a membrane-disruptive tendency of PEG-lipid at high concentration, 5 to 10% of it in a liposome appears both compatible with vesicle morphology and technologically useful. Indeed, “stealth” liposomes formed with PEG-lipid and injected into the bloodstream have been found to be cleared more slowly from the blood circulation than conventional liposomes (2). As a result of this extended circulation time, stealth vesicles loaded with anticancer drugs (e.g., doxorubicin) circulate long enough to find their way into well-hidden tumors. This may work because blood plasma proteins, which generically adsorb to artificial surfaces and mediate clearance by immune system cells, are sterically delayed in deposition either into or onto the “stealth” membranes by the PEG chains (19).

Solvent, Size, Energetics, and Fluidity

In organic solvents and multi-component solutions as complex as blood plasma, transitions between aggregate morphologies as well as aggregate fluidity and stability are governed by chain MW , interfacial tensions, and/or selective interactions with one preferred

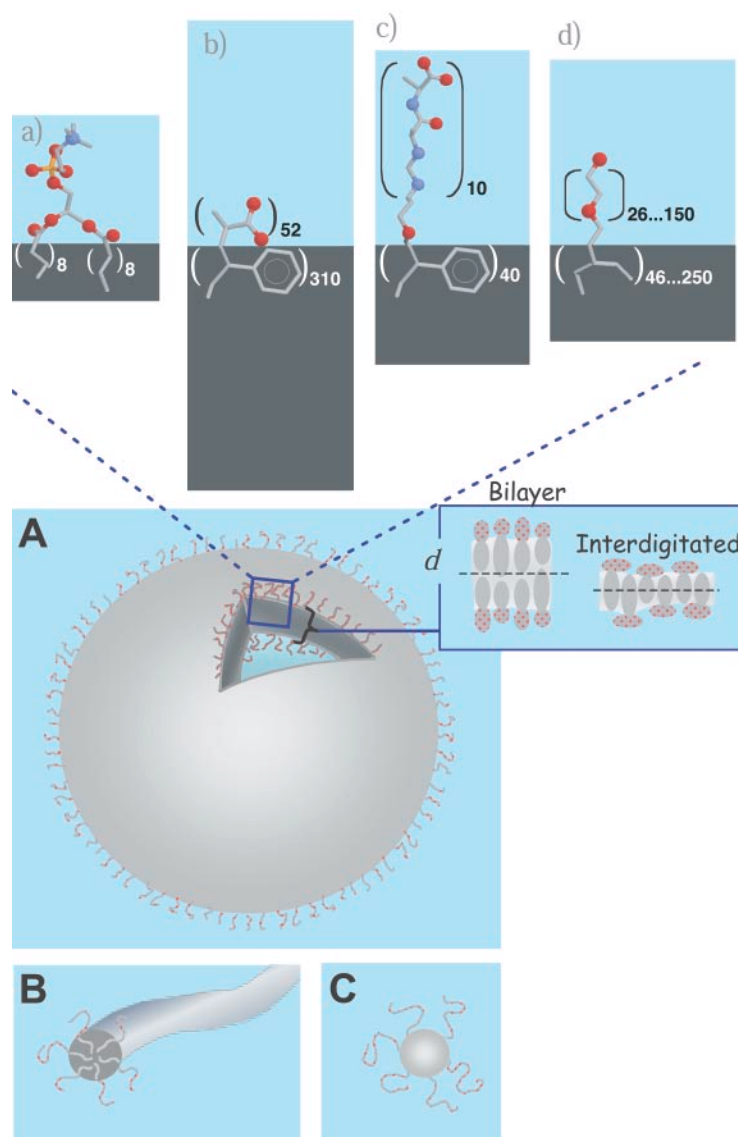


Fig. 1. Schematic of a vesicle and related micellar aggregates plus vesicle-forming lipid and diblock copolymers. (A) Vesicle with a section removed to reveal the membrane thickness d , schematically represented by the dark gray regions for (a) a phosphatidylcholine lipid as a typical, natural liposome former; (b) a diblock copolymer of polyacrylic acid–polystyrene (PAA-PS), which precipitates as a vesicle when water is added to solvent (24); (c) PS–poly(isocyanol-alanine-L-alanine), which makes vesicles in coexistence with rods under acidic conditions (30); and (d) a molecular weight series of nonionic polyethyleneoxide–polybutadiene (PEO-PBD), which makes robust vesicles in pure aqueous solutions (37–38). In these physical representations of amphiphile structure, gray is hydrocarbon, red is oxygen, blue is nitrogen, and yellow is phosphorus. Detailed chemical structures are given in the references; note that the numbers of monomer units indicated for the block copolymers are just average numbers. As sketched in cross section, a vesicle membrane can be a bilayer with a well-defined midplane, as is typical of phospholipid membranes, or it can be a more interdigitated structure. Polydispersity in molecular size that is intrinsic to polymer amphiphiles would tend to give a more intermediate membrane structure. (B and C) A worm- or rod-like micelle and a spherical micelle, respectively, formed from block copolymers and related amphiphiles.

fraction of the amphiphile (20). Phospholipids segregate and form vesicles in many aqueous solutions, for example, but they fail to do so in solvents that are blind to their amphiphilicity (e.g., chloroform). Solubility also depends in general on chain MW , which suggests that novel vesicles can also be made by aggregation of weakly hydrophobic polymers.

Lipids and small amphiphiles can differ considerably in their hydrophilic head group, but they almost always contain one or two strongly hydrophobic chains composed of multiple ethylene units ($-\text{CH}_2-\text{CH}_2-$)_{*n*} (with $n = 5$ to 18 typically). A simple measure of vesicle stability is provided by the critical micelle concentration $C_{\text{CMC}} \sim \exp(-n\epsilon_h/k_B T)$, where $k_B T$ is the thermal energy and ϵ_h is the monomer's effective interaction energy with the bulk solution. Only at surfactant concentrations above C_{CMC} do aggregates such as vesicles form. For ethylene groups at biological T_{biol} , $\epsilon_h \approx 1$ to 2 $k_B T_{\text{biol}}$ (~ 4 to 8 pN·nm) so that values of C_{CMC} for lipids and related amphiphiles in aqueous solutions range from micromolar to picomolar (i.e., aggregates are stable in high dilution). Amphiphile exchange rates between aggregates are also generally proportional to C_{CMC} , with characteristic exchange times for phospholipids estimated in hours. Polymer amphiphiles with hydrophobic MW_h larger than those typical of lipids by an order of magnitude or more result in kinetic quenching and metastable aggregates. Such effects motivate investigations of cosolvents that fluidize and activate the polymer systems (e.g., by reducing ϵ_h).

Many responses of the assembled aggregates are predicated not on n or MW but on the most interfacial hydrophobic monomers, because these monomers see both head group moieties and bulk solution. As a result, interfacial monomers typically have screened interface energies $\epsilon_i \leq \epsilon_h$. Thus, on the scale of the monomer area a (~ 0.5 nm² for lipid in water), the interfacial tension that is created has a magnitude $\gamma \approx \epsilon_i a^{-1}$, which is invariably much less than the ~ 70 mN/m between water and air. This tension is balanced by fluid-like packing interactions (21) and suggests that vesicle formation processes as well as vesicle shapes—like the varied shapes of cells (1)—are generally influenced by hydrodynamic-type forces such as mechanical shear. Entangled and glassy polymers can be expected, however, to slow down lateral or in-plane rearrangements of molecules (i.e., convection and diffusion) and thereby impede morphological responses of polymer vesicles.

Despite the potential for nonequilibrium flow effects, a molecular-scale force balance is also expected to underlie the basic stability of a curved, vesicular aggregate, just as domed buildings must balance their internal stresses in defying collapse under gravity. In place of gravity, however, os-

motonic pressure (allowed by a vesicle's semipermeable membrane) largely dictates vesicle volume up to the point of actually tensing the vesicle's membrane (21). Assuming no osmotically induced tension and a simple spherical vesicle of radius R , the local curvature nonetheless leads to a slight molecular splay and a change in exposed area Δa , which is often considered dependent on the square of the membrane thickness d . The associated cost $\gamma \Delta a$ generates a local curvature energy classically viewed as proportional to $1/R^2$ (21). Integrated over a vesicle area $4\pi R^2$, however, the total curvature energy, $F_c \propto \gamma d^2 4\pi R^2 \times 1/R^2$, is independent of R . From this perspective, vesicle size in a given solution thus depends less on thermodynamics and more on nonequilibrium aspects of the formation process.

In addition to the classical curvature energy above, vesicle bilayers as well as multilamellar vesicles embedded one within the other like an onion can also have a strain energy, analogous to that in a bimetallic strip held flat while heated. The lateral strain that arises from a mismatched number of molecules in one leaflet or layer relative to the other(s) leads to an area difference elasticity (22). "Flip-flop" of amphiphiles from one monolayer leaflet to another relaxes the strain. In cells the process is catalyzed by specific proteins called "flipases" (23), which underscore the cost of transferring the hydrophilic part of an amphiphile through a membrane's hydrophobic core. However, because synthetic polymers are polydisperse in MW , a small fraction of less hydrophilic chains are more prone to flip-flop. In addition, provided one is not strictly focused on pure aqueous systems, cosolvents can also be used to swell and fluidize the membrane core, helping to minimize the cost of transfer between leaflets.

Vesicles from Large Block Copolymers: Solvent Effects and Flip-flop Stabilization

Illustrative of the challenges surmounted with select copolymer systems, vesicles can be formed from diblocks in which the hydrophobic segment not only has a high glass transition temperature (e.g., polystyrene, PS), and the hydrophilic segment is ionic [e.g., poly(acrylic acid), PAA], but the overall copolymer molecular weight (i.e., $MW \gg 10$ kD) is also considerably higher than that of lipids (17). For the representative system PS₃₁₀-PAA₅₂ (Fig. 1A, b), vesicle preparation needs to be carried out indirectly—that is, by first dissolving the diblock in a solvent suited to both blocks (dioxane) and then adding water as a precipitant. The water drives PS aggregation and increasingly establishes an interfacial tension. Solvent changes also tend to alter the preferred polymer geometry

and lead to a morphological evolution from spheres to rods to vesicles as water is added (Fig. 2A) (24).

Within the relatively expansive vesicle phase, as more water is added, the hydrophobic (PS) block increasingly avoids hydration and γ goes up, tending to straighten the interface and increase R . Single-walled or unilamellar vesicles thus undergo a reversible change in size from $R \sim 45$ to 100 nm as water content is changed from 25 to 70% (Fig. 2B). However, the wall thickness d appears to stay nearly constant and implies an increase in the mass of any given vesicle.

Preferential swelling and fluidization of the membrane by the organic solvents (25) as well as vesicle ripening processes predicated on copolymer solubility (C_{CMC}) might all contribute to vesicle growth, but fusion and fission are also apparent in images of quenched systems (Fig. 2C). From these, the fusion process seems very fluid in the sense that lateral rearrangements of molecules must be occurring to generate predominantly spherical shapes (Fig. 2B). Indeed, contact and adhesion of vesicles would appear to be followed by coalescence and formation of a central, connecting wall. Destabilization of the wall leads to its asymmetric detachment and retraction with final formation of a uniform outer wall. The reverse (fission) process starts with elongation of the vesicle, formation of an internal waist, narrowing of the external waist, and final complete separation. The resemblance to biological processes involving cell membranes is obvious. Vesicle fusion and fission kinetics have been followed by turbidity changes after jumps in water content and are found to have relaxation times as fast as seconds (26), which clearly implies a high wall fluidity.

Consistent with fluidized walls, molecular flip-flop associated with polymer polydispersity (in both MW and f) also appears to enter into both curvature stabilization and relaxation. Short chains will tend to segregate to the inside of a vesicle, whereas long chains will stay on the outside (27). The resulting segregation of corona chains induces different repulsion strengths (steric and/or electrostatic) on the two sides of the bilayer, tending to thermodynamically stabilize a unique value of R . Segregation has proven to be reversible and most pronounced for small vesicles (28), consistent with the expected curvature dependence in an area-difference elasticity mechanism (22). Two different types of polymer chains can also be localized on the inside and the outside of the vesicles if the corona blocks are of sufficiently different lengths, as shown with PS-PAA and related diblocks (29). Thus, if suitable fluidizing solvents are used, large block copolymers are able to equilibrate as a result of relatively high fluidity at both the molecular level (flip-flop) and the whole-vesicle level (i.e., fusion and fission).

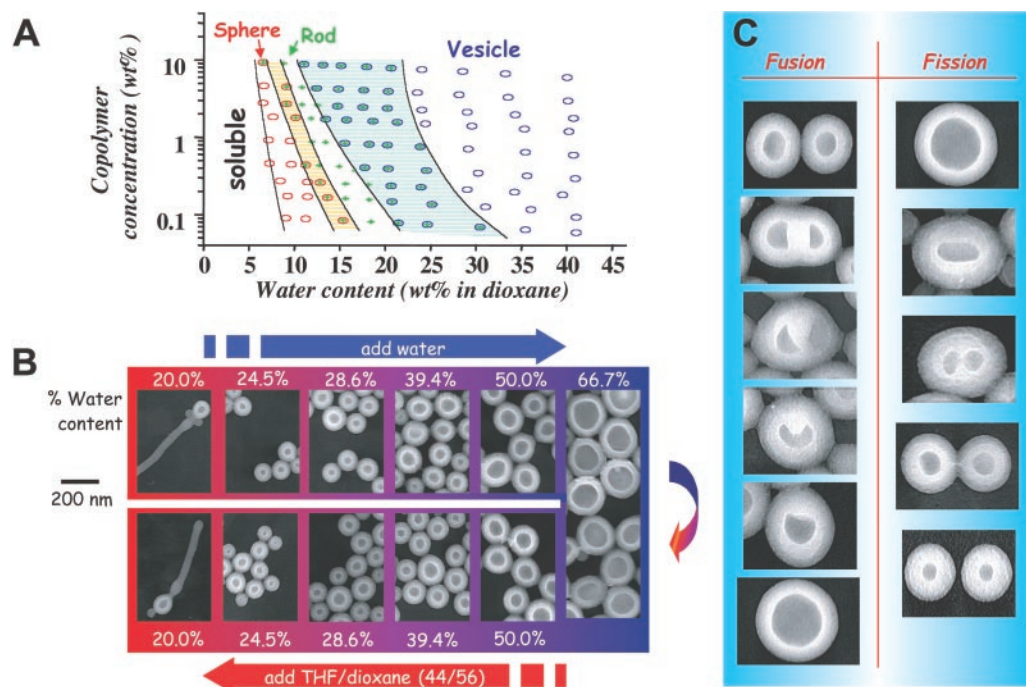


Fig. 2. Morphological phases and vesicle transformations in dilute solutions. **(A)** Phase diagram of PS_{310} - PAA_{52} in dioxane plus water; the full ternary phase diagram with separate water, dioxane, and copolymer axes looks similar (24). The colored regions between sphere and rod phases and between rod and vesicle phases correspond to coexistence regions. **(B)** Reversibility of the vesicle formation and growth process for PS_{300} - PAA_{44} (28), presumably based in part on fusion and fission processes illustrated in **(C)**.

Polymersomes from Block Copolymers in Aqueous Solutions

Extending many years of experience in the manufacture and characterization of liposomes, diblock copolymer vesicles have also been made and studied in strictly aqueous solutions. Unlike the precipitated shells above, which clearly illustrate aggregate assembly but otherwise use highly asymmetric diblocks ($f_{\text{hydrophilic}} < 20\%$) and have many uncharacterized properties (e.g., solvent distribution or stability in purely aqueous solution), the vesicles reviewed below have so far involved the use of shorter and/or less glassy copolymers. Nonetheless, MW s are still far greater than those of lipids. Maintaining the stability of potential encapsulants or surface modifiers such as folded proteins is one important practical motivation, as discussed below.

The dipeptide construct PS_{40} -poly(isocyanate-L-alanine-L-alanine) $_m$ (Fig. 1A, c) is an early example of a diblock that assembles directly under solvent-free aqueous conditions (30). It is semisynthetic in the sense that it contains naturally occurring peptide moieties—a design expanded upon in recent years. Under mildly acidic conditions and for $m = 10$ (but not $m = 20$ or 30), collapsed vesicular shells tens to hundreds of nm in diameter were observed coexisting with rod-like filaments and chiral superhelices (recall the coexistence region in Fig. 2A).

With the use of fully synthetic diblock

copolymers of PEO_m - PBD_n (PBD, polybutadiene) (Fig. 1A, d) and the hydrogenated homolog PEO -polyethylene (PEO_m - PEE_n), more monomorphic, unilamellar vesicles referred to as “polymersomes” have been made under a variety of aqueous conditions (31–38). Figure 3A shows how addition of water to a lamellar (15) film, micrometers thick, generates polymersomes. Initial quantitative studies of small solute (e.g., doxorubicin) and protein encapsulation (36) during hydration indicate efficiencies comparable to liposomes and suggest the potential for novel polymer-based controlled-release vesicle systems.

On the basis of the examples above (and more below), one unifying rule for polymersomes in water is a phospholipid-like ratio of hydrophilic to total mass: $f_{\text{hydrophilic}} \approx 35\% \pm 10\%$ (35). A cylindrically shaped molecule that is asymmetric with $f_{\text{hydrophilic}} < 50\%$ presumably reflects the ability of hydration to balance a disproportionately large hydrophobic fraction. Molecules with $f_{\text{hydrophilic}} > 45\%$ can be expected to form micelles, whereas molecules with $f_{\text{hydrophilic}} < 25\%$ can be expected to form inverted microstructures. Sensitivities of these rules to chain chemistry and MW have not been fully probed, but copolymers following these rules and yielding polymersomes have thus far had MW s ranging from ~ 2700 to 20,000 g/mol. Moreover, cryogenic transmission electron microscopy (cryo-TEM) of 100- to 200-nm vesicles shows that membrane cores increase

with MW from $d \approx 8$ to 21 nm (35, 37, 38). Lipid membranes have a far more limited range of $d \approx 3$ to 5 nm, which is clearly compatible with the many integral membrane proteins in cells. Polymersome membranes thus present a novel opportunity to study membrane properties as a function of d (or MW).

MW -Dependent Properties of Polymersomes

Retention of encapsulants (e.g., dextrans, sucrose, physiological saline) over periods of months has been observed with ~ 100 -nm polymersomes prepared by liposome-type extrusion techniques (32, 33) as well as with ~ 10 - μm giant vesicles (Fig. 3A). The latter allow detailed characterization by single vesicle micromanipulation methods (21, 39) (Fig. 3B). Lateral diffusivity (36) as well as apparent membrane viscosity (35, 38) indicate that membrane fluidity (distinct from flip-flop) decreases with increasing MW . Moreover, the decreases are most drastic when the chains are long

enough to entangle. Area elasticity measurements of γ (~ 25 mN/m) appear independent of MW and indicate that opposition to interface dilation is dictated by polymer chemistry and solvent alone. Electromechanical stability increases with membrane thickness up to a limit reflective of γ (35, 37, 38). Phospholipid membranes rupture well below such a limit simply because their small d makes them more susceptible to fluctuations and defects. To exceed this interfacial limit of any self-assembly, one must introduce additional interactions such as covalent crosslinking within the membranes (40–42)—an idea long recognized (3) but only rarely realized even with small liposomes (4). Permeation of water through the polymersome membranes has begun to be measured (31) and shows, in comparison to phospholipid membranes, a considerably reduced transport rate. This is consistent with early measurements on liposomes by Bangham on a relatively narrow MW -series of lipids (5). What appears most suggestive from the studies to date is that biomembranes are optimized less for stability than for fluidity. In this context, cholesterol is an intriguing component of cell membranes because it both toughens and fluidizes (1).

Several triblock copolymers also appear to fall within the class of polymersome-formers, and differences in membrane properties offer important insights. At least one commercial triblock known as a “pluronic” with a relatively large poly(propyleneoxide) mid-

block (PEO₅-PPO₆₈-PEO₅) yields small vesicles in water with relatively thin membranes of $d = 3$ to 5 nm and stability of only hours (43). Such results likely reflect the weakly hydrophobic midblock PPO and the interfacial localization of the midblock's oxygens.

Indeed, factoring the oxygen into an effective hydrophilic fraction shows that this vesicle-forming superamphiphile has an $f_{\text{hydrophilic}}$ in the same range as lipids. Another vesicle-forming triblock with a lipid-like $f_{\text{hydrophilic}}$ (~40%) consists of a hydrophobic midblock of poly(dimethylsiloxane) (PDMS) and two water-soluble blocks of poly(2-methyloxazoline) (PMOXA) terminating in cross-linkable methacrylate groups (41, 42). The polydispersity in MW of this copolymer is notably broad (41, 42) and implies that polydispersity is not a severe limitation to vesicle formation. A first example of a vesicle-forming pentablock composed of PEO and a polysilane (44) is also intriguing, although the electron microscopy is thus far suggestive of incomplete, collapsed shells.

Increased functionality of self-assembling block copolymers is a desired feature of emerging polymersome systems. These include suitably proportioned copolymers of PEO-poly(propylenesulfide) (PEO-PPS) whose PPS blocks are susceptible, in principle, to oxidative degradation (45). Kilo-dalton-size large block copolymers of PEO-poly(lactide) (PEO-PLA) are known to make micelles (46) and are of great interest because PLA is susceptible to hydrolytic biodegradation, as widely exploited in the field of controlled drug release [(e.g., (47)]. Hence, biodegradable vesicles for controlled release of encapsulants seem achievable, and preliminary results indicate that this is indeed feasible if $f_{\text{hydrophilic}}$ is lipid-like (48).

Vesicles in Industry

Vesicle development has perhaps been most prominent in the cosmetics and pharmaceutical industries, with progress in the latter predicated on years of phased testing and governmental approval. Nonetheless, both stealth and conventional liposomes loaded with anticancer agents have overcome cost, scale-up, sterility, and stability hurdles, and have also demonstrated clinical efficacy (2). For topical or cosmetic application, novosomes are perhaps the latest multilamellar incarnation of the earlier synthetic niosomes and are reported to have the processability of many simple emulsifications (49). The polymer processing and materials revolution of the 20th century might likewise extend to vesicle encapsulators of the future.

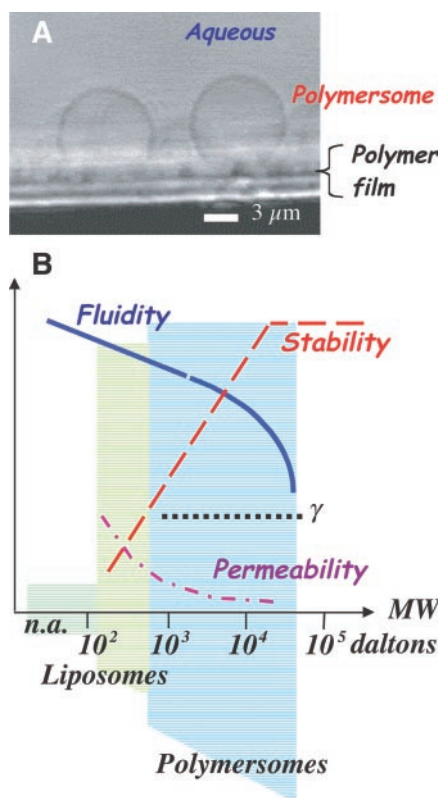


Fig. 3. Polymersome formation and membrane property trends. **(A)** Analogous to liposomes, diblock copolymer vesicles can be formed by hydration of a thin, dried film of copolymer (32, 33). Aqueous solutions can vary from phosphate-buffered saline to 1 M sucrose or distilled water. **(B)** Schematic of membrane properties versus amphiphile molecular weight based on single vesicle measurements; n.a. denotes non-aggregating systems. Liposomes and related vesicles are generally made with amphiphiles with MW less than 1 kD; polymersomes can be made in aqueous solution with larger amphiphiles. Difficulties at high MW might be attributed to a rapid decrease in fluidity associated with entangling chains (35–38). At least for strongly segregating diblocks, the membrane thickness increases with MW and makes polymersomes decreasingly permeable. Stability by a number of measures also increases, but only up to a limit set by the interfacial tension that drives membrane formation.

systems may not be so large a region in a suitable phase diagram (e.g., Fig. 2A with both ionic strength and pH axes added). Diblocks of poly(ethylene)-poly(styrene-sulfonic acid) (PEE-PSSH) are prime candidates to study polyelectrolyte effects (51), but many additional charged block copolymers and mixtures are conceivable.

Templated shells of layered polyelectrolytes (52) might, for example, inspire new vesicle designs.

The effects of chain flexibility in vesicle membranes are also not yet clear. In lamellar phases of pure block copolymers, chains tend to be laterally squeezed and effectively stretched by the interfacial tension. Polymers also have an instantaneous major axis (like any liquid crystal molecule) and packing tends to align adjacent axes. Either effect gives fractal scaling for $d \sim MW^b$, with $b = 0.5$ to 0.66 (13); rod-like polymers have $b = 1$. One diblock of note (53) uses rigid ring monomers of phenylquinoline (PQ) to make a rod-coil copolymer with PS (specifically, PS₃₀₀-PPQ₅₀), which gives collapsed monolayer shells (rather than the bilayer or interdigitated membranes of Fig. 1A) when precipitated out of solvent. One feature of interest with this system is a novel photoluminescent coupling in the PPQ that arises in an aggregate-specific manner. More generally, however, this diblock suggests the vesicle-forming potential of stiff, rod-like chains, although one difficulty that might be anticipated with long, stiff hydrophobic blocks is the inability of a membrane sheet to bend and seal its edges for all but the largest, giant vesicles.

Interfacing with Biological Structures and Functions

In a somewhat surprising result, integral membrane proteins 3 to 5 nm high have been compatibly inserted into PDMS-PMOXA membranes ($d \approx 10$ nm) (54). At least two features of polymer membranes facilitate protein miscibility (55): (i) Polymer chains can be compressed considerably, and (ii) polydispersity allows small chains to segregate around a membrane protein. Inserted channel proteins can also effectively dock with viruses and facilitate transfer-loading of viral DNA into the polymer vesicle (Fig. 4A) (56). DNA delivery would, of course, seem important to explore if release mechanisms can be incorporated. From a fundamental perspective as well, the broadened osmotic and rupture characteristics of polymer vesicles might be used to confirm emerging estimates of internal pressures exerted by encapsulated DNA.

Extending their work on dipeptide-containing block copolymers (30), Nolte and co-workers have covalently attached a PS₄₀ chain to an enzymatically active water-soluble protein of $MW = 40$ kD ($f_{\text{hydrophilic}} \sim 50\%$) (Fig. 4B). In solution, the conjugate generated worm-like micelles (57). Longer chains of PS_{60–80} might be required to obtain vesicles or sheets, but, the general idea is clearly to have multienzyme scaffolds in which en-

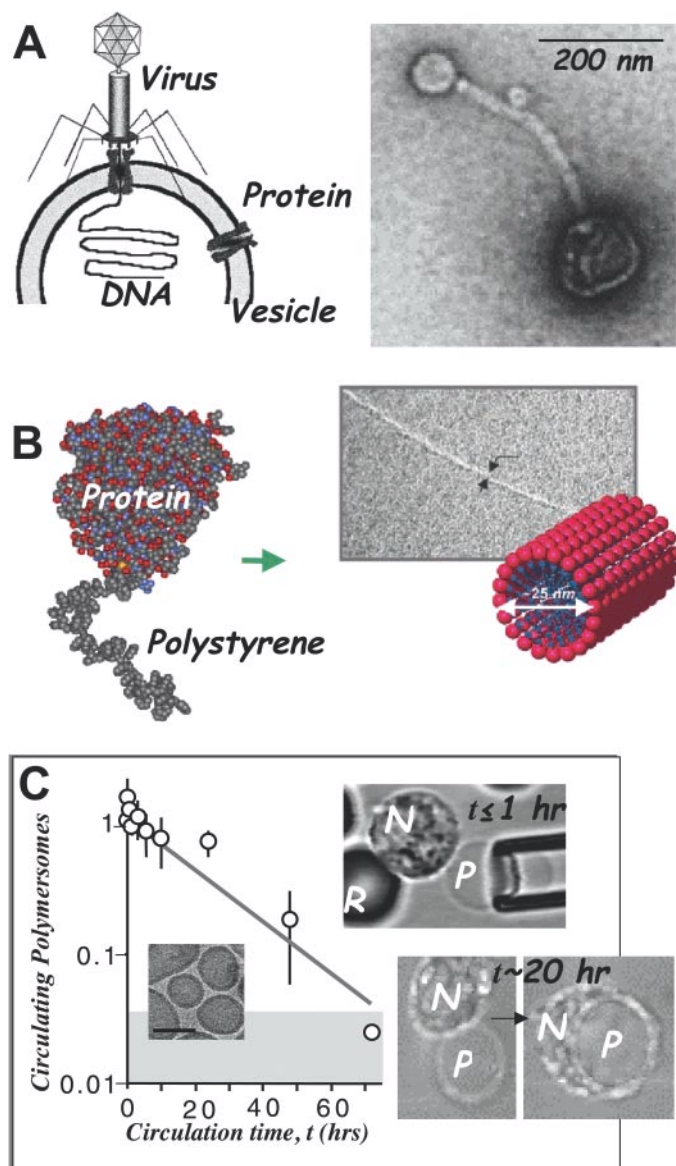


Fig. 4. Polymer amphiphile systems at the interface with biology. (A) Virus-assisted loading of a triblock copolymer vesicle containing a natural channel protein in its membrane (56); for liposomes, see (60). (B) Protein-polymer hybrid amphiphile that assembles in a tetrahydrofuran (THF)-water solution into rod-like micelles 25 nm in diameter (57). (C) Biocompatibility studies of PEO-based polymersomes (32, 33, 61). The exponential decay in circulating polymersomes in a rat model indicates a circulation half-life comparable to times found for stealth liposomes (2). The inset below the curve is a cryo-TEM image of ~ 100 nm (scale bar) polymersomes. The two optical micrographs at right show giant polymersomes, P, placed in contact with a phagocytic neutrophil, N, by a micropipette (of diameter $5 \mu\text{m}$). R denotes a red blood cell. The vesicles were preincubated in plasma for the indicated times, and only after tens of hours were the polymersomes engulfed by the phagocytic neutrophils.

zyme A passes its product to adjacent enzyme B and so on, cooperating in a localized metabolic chain. Photosynthesis and polypeptide extension by ribosomes are just two among many biological reactions that exploit enzymatic proximity. A synthetic cell that senses and enzymatically acts on its environment, like a biomembrane's glycocalyx does (1), might also be developed around these biohybrid superamphiphiles.

can be faithfully mimicked by synthetic polymer vesicles (e.g., protein integration, fusion, DNA encapsulation, compatibility). It also appears clear that biomembranes are not optimized for either stability or equilibrium; they do not need to be, because they encapsulate ample machinery to maintain a dynamic, animated state. Perhaps the most useful concept to mimic and extend with block copolymers is the am-

phiphilicity template provided by lipids. In light of the material versatility of polymers in terms of their molecular weight, polydispersity, reactivity, and synthetic diversity, a strictly polymer approach to vesicles would seem to offer many possibilities.

In a more complex biological milieu, polymersomes are also showing initial promise. Injection of ~ 100 -nm PEO-PEE polymersomes (32, 33) into the blood circulation of rats yields results (Fig. 4C) similar to those for stealth liposomes, which circulate for ~ 15 to 20 hours and end up being engulfed by phagocytic cells of the liver and spleen (2). Parallel test tube studies involving timed preincubations in cell-free blood plasma (Fig. 4C, inset) help to elucidate the delayed, liposome-like clearance mechanism whereby plasma protein slowly accumulates on the polymersome membrane (19) and eventually mediates cell attachment. The PEO brush provides an effective delay to this process and thus acts somewhat like a biomembrane glycocalyx (1). Such results highlight the biomedical promise of polymersomes.

Lessons Learned

With the increasing exploration and development of polymer vesicle systems, one underlying goal is to expand on and clarify the properties of natural cell systems that have evolved over

cons. It is already clear that many biological membrane processes

References and Notes

1. R. Lipowsky, E. Sackmann, Eds., *Structure and Dynamics of Membranes—from Cells to Vesicles* (Elsevier Science, Amsterdam, 1995).
2. D. D. Lasic, D. Papahadjopoulos, Eds., *Medical Applications of Liposomes* (Elsevier Science, Amsterdam, 1998).
3. H. Ringsdorf, B. Schlarb, J. Venzmer, *Angew. Chem. Int. Ed.* **27**, 113 (1988).
4. S. C. Liu, D. F. O'Brien, *J. Am. Chem. Soc.* **124**, 6037 (2002).
5. A. D. Bangham, *Chem. Phys. Lipids* **64**, 275 (1993).
6. B. Cornet, E. Decroly, D. Thines-Sempoux, J. M. Ruysschaert, M. Vandenbranden, *AIDS Res. Hum. Retroviruses* **8**, 1823 (1992).
7. Reviewed in I. F. Uchegbu, Ed., *Synthetic Surfactant Vesicles: Niosomes and Other Non-Phospholipid Vesicular Systems*, vol. 11 of *Drug Targeting and Delivery* (Harwood Academic, Amsterdam, 2000).
8. S. Q. Zhou et al., *Science* **291**, 1944 (2001).
9. J. C. M. van Hest, D. A. P. Delnoye, M. W. P. L. Baars, M. H. P. van Genderen, E. W. Meijer, *Science* **268**, 1592 (1995).
10. H. T. Jung, B. Coldren, J. A. Zasadzinski, D. J. Iampietro, E. W. Kaler, *Proc. Natl. Acad. Sci. U.S.A.* **98**, 1353 (2001).
11. F. S. Bates, G. H. Fredrickson, *Phys. Today* **52**, 32 (1999).
12. S. Förster, M. Zisenis, E. Wenz, M. Antonietti, *J. Chem. Phys.* **104**, 9956 (1996).
13. Early theory can be found in (58).
14. Förster et al., *Macromolecules* **34**, 4610 (2001).
15. D. A. Hajduk, M. B. Kossuth, M. A. Hillmyer, F. S. Bates, *J. Phys. Chem. B* **102**, 4269 (1998).
16. J. Israelachvili, *Intermolecular and Surface Forces* (Academic Press, New York, ed. 2, 1991).
17. L. Zhang, A. Eisenberg, *Science* **268**, 727 (1995).
18. F. K. Bedu-Addo, P. Tang, Y. Xu, L. Huang, *Pharm. Res.* **13**, 710 (1996).
19. S. C. Semple, A. Chonn, P. G. Cullis, *Adv. Drug Delivery Rev.* **32**, 3 (1998).
20. K. J. Hanley, T. P. Lodge, C. I. Huang, *Macromolecules* **33**, 5918 (2000).
21. E. A. Evans, R. Skalak, *Mechanics and Thermodynamics of Biomembranes* (CRC Press, Boca Raton, FL, 1980).
22. H. G. Döbereiner, E. Evans, M. Kraus, U. Seifert, M. Wortis, *Phys. Rev. E* **55**, 4458 (1997).
23. C. F. Higgins, *Cell* **79**, 393 (1994).
24. H. Shen, A. Eisenberg, *J. Phys. Chem. B* **103**, 9473 (1999).
25. I. A. Maxwell, J. Kurja, *Langmuir* **11**, 1987 (1995).
26. A. Choucair, A. Kycia, A. Eisenberg, in preparation.
27. L. Luo, A. Eisenberg, *J. Am. Chem. Soc.* **123**, 1012 (2001).
28. ———, *Langmuir* **17**, 6804 (2001).
29. ———, *Angew. Chem. Int. Ed.* **41**, 1001 (2002).
30. J. J. L. M. Cornelissen, M. Fischer, N. A. J. M. Sommerdijk, R. J. M. Nolte, *Science* **280**, 1427 (1998).
31. B. M. Discher et al., *Science* **284**, 1143 (1999).
32. J. C.-M. Lee et al., *Biotech. Bioeng.* **43**, 135 (2001).
33. The hydrophobic PBD and PEE blocks studied are closely related to biocompatible polyprenyl chains found ubiquitously in animal and plant membranes (34).
34. I. Eggens, T. Chojnacki, L. Kenne, G. Dallner, *Biochim. Biophys. Acta* **751**, 355 (1983).
35. H. Aranda-Espinoza, H. Bermudez, F. S. Bates, D. E. Discher, *Phys. Rev. Lett.* **87**, 208301 (2001).
36. J. C.-M. Lee, M. Santore, F. S. Bates, D. E. Discher, *Macromolecules* **35**, 323 (2002).
37. R. Dimova, U. Seifert, B. Pouligny, S. Förster, H.-G. Döbereiner, *Eur. Phys. J. E* **7**, 241 (2002).
38. H. Bermudez et al., *Macromolecules*, in press.
39. M. Bloom, E. Evans, O. G. Mouritsen, *Q. Rev. Biophys.* **24**, 293 (1991).

40. B. M. Discher *et al.*, *J. Phys. Chem. B* **106**, 2848 (2002).
41. C. Nardin, T. Hirt, J. Leukel, W. Meier, *Langmuir* **16**, 1035 (2000).
42. Polydispersities are generally reported as weight-average MW divided by number-average MW ; typical ratios for the copolymers of Fig. 1 are ~ 1.05 to 1.15 . A value of 1.7 was reported for the triblock copolymer of (41).
43. K. Schillen, K. Bryskhe, Y. S. Mel'nikova, *Macromolecules* **32**, 6885 (1999).
44. N. A. J. M. Sommerdijk, S. J. Holder, R. C. Hiorns, R. G. Jones, R. J. M. Nolte, *Macromolecules* **33**, 8289 (2000).
45. A. Napoli, N. Tirelli, G. Kilcher, J. A. Hubbell, *Macromolecules* **34**, 8913 (2001).
46. R. P. Batycky, J. Hanes, R. Langer, D. A. Edwards, *J. Pharm. Sci.* **86**, 1464 (1997).
47. S. A. Hagan *et al.*, *Langmuir* **12**, 2153 (1996).
48. PEO-PLA vesicles have been observed with a copolymer having $f_{\text{PEO}} \approx 33\%$ and $MW \approx 6$ kg/mol (59).
49. R. Mathur, P. Capasso, *ACS Symp. Ser.* **670** (1995), p. 219.
50. J. M. Gebicki, M. Hicks, *Nature* **243**, 232 (1973).
51. M. Regenbrecht, S. Akari, S. Forster, H. Mohwald, *J. Phys. Chem. B* **103**, 6669 (1999).
52. F. Caruso, D. Trau, H. Mohwald, R. Renneberg, *Langmuir* **16**, 1485 (2000).
53. S. A. Jenekhe, X. L. Chen, *Science* **279**, 1903 (1998).
54. W. Meier, C. Nardin, M. Winterhalter, *Angew. Chem. Int. Ed.* **39**, 4599 (2000).
55. N. Dan, S. A. Safran, *Macromolecules* **27**, 5766 (1994).
56. A. Graff, M. Sauer, P. V. Gelder, W. Meier, *Proc. Natl. Acad. Sci. U.S.A.* **99**, 5064 (2002).
57. K. Velonia, A. E. Rowan, R. J. M. Nolte, *J. Am. Chem. Soc.* **124**, 4224 (2002).
58. E. Helfand, in *Developments in Block Copolymers*, Z. R. Wasserman, Ed. (Applied Science, New York, 1982), chapter 4.
59. F. Ahmed, I. Omaswa, A. Brannan, F. S. Bates, D. E. Discher, in preparation.
60. O. Lambert, L. Letellier, W. M. Gelbart, J.-L. Rigaud, *Proc. Natl. Acad. Sci. U.S.A.* **97**, 7248 (2000).
61. P. Photos, B. M. Discher, L. Bacakova, F. S. Bates, D. E. Discher, in preparation.
62. Support for our work and interest (D.E.D.) in polymer vesicles was provided by the NSF Materials Research Science and Engineering Center (MRSFC) at the University of Pennsylvania and by an NSF-PECASE award (D.E.D.).

REVIEW

How Surface Topography Relates to Materials' Properties

Hazel Assender, Valery Bliznyuk,* Kyriakos Porfyrakis

The topography of a surface is known to substantially affect the bulk properties of a material. Despite the often nanoscale nature of the surface undulations, the influence they have may be observed by macroscopic measurements. This review explores many of the areas in which the effect of topography is macroscopically relevant, as well as introducing some recent developments in topographic analysis and control.

Those few materials whose surface is atomically flat are of great use to scientists and for certain technological applications; however, the majority of materials have a surface landscape made up of undulations and even perhaps steep gradients and pores. These constitute the topography of the surface, a property that is often difficult to define by a few simple parameters but nevertheless can have a considerable impact on a material's performance. Such importance reflects the surface-specific nature of many properties: the ability to adhere to another material, optical properties, or tribology, for example.

Issues of topography are perhaps particularly pertinent in the case of soft matter. For instance, the size of typical topographic features may be comparable with the molecular dimension and, for some technologies, with the thickness of the soft layer itself. Soft matter allows the use of a number of specific methods to manipulate topography, and in the kinds of applications in which soft matter is employed, the topography is often of specific importance. For example, for food packaging, a compliant adhesive layer might be used to smooth the surface of a polymer substrate

before the deposition of a gas barrier layer (1). Similarly, the electro-optical behavior of thin films of polymers used in electronic devices has been shown to correlate with their topography (2, 3).

The correlation between surface structure and properties is important within two broad areas of considerable recent interest in materials science. The first is in the realm of biological and biomedical materials, in which the shape of a surface controls its interaction with biological components; for example, whether bacteria will grow on a particular surface—a subject of interest to anyone who wishes to keep surfaces hygienic or their teeth clean! The second important developing area is that of nanocomposites and nanostructured materials, which frequently combine soft matter with metals or ceramics for applications as diverse as electronics, packaging, and information storage. When combining materials on scales in the range from 10 nm to 1 μm (and these include many that are found in biology), the interface becomes of substantive importance to the materials' performance; and the topography of the interface, or the surface as a precursor to an interface, may be on a comparable scale to that of the nanostructured material.

The Origin of Topography

Topography may be induced at the surface of soft matter by its inherent relaxation or, more actively for example, by the exploitation of mixtures of materials, mechanical roughening, chemical patterning, or even electric fields.

When allowed to relax at its surface, soft matter will form surface undulations, known as capillary waves, as a result of the inherent entropy of the system balancing the increased energy of the greater surface area (4). The relatively low surface energy of molecular materials combined with their compliance makes such an effect important in soft materials. The addition of an electric field can lead to electrohydrodynamic instabilities and consequent patterning of a viscous polymer film (5).

One example is shown in Fig. 1, where a thin polystyrene film [capped with an ultrathin (flexible) Al layer as an electrode] has dewetted an Al-coated substrate after application of an electric field of strength 5.7×10^7 V m⁻¹ (6). One possible application of layers that have artificially induced topography such as this might be the creation of antireflective coatings in which the roughened surface scatters the reflected light (7). Where block copolymers are used, such nanopatterning may be controlled by the phase structure resulting from two-dimensional (2D) viscous flow as the structure orders, and it also may be influenced by the topography of an underlying substrate (8). Electric fields may also influence the patterning formed in these copolymer systems (9). Similarly, thin films of blends may be exploited to produce a surface topography resulting from phase separation processes (10). In addition, chemical patterning of a surface may lead to preferential phase separation to induce nanopatterning in the topography of a subsequent layer (11). Many impressive structures have been reported, and the whole area of nanopatterning, nanolithography, and self-organizing layers is an area of current great excitement. We await further developments in the practical exploitation of such systems and in the degree to which they may be controlled on a more substantial scale.

Department of Materials, University of Oxford, Parks Road, Oxford OX1 3PH, UK.

*Present address: Department of Construction Engineering, Materials Engineering, and Industrial Design, Western Michigan University, Kalamazoo, MI 49008, USA.